# Decorated Graphene Model 1

Following the 2018 discovery of superconductivity in twisted bilayer graphene [1], graphene-based systems gained a renewed interest as a platform for strongly correlated physics. Two methods to engineer strong electron correlations emerged: twisted multilayer systems [1–5] and multilayer systems without twisting, such as Bernal bilayer, ABC or ABCA layered systems [6]. Through different means, electrons in these systems become localized so that interaction effects get more strongly pronounced. Connecting both kind of systems is the strong quantum geometry coming from the graphene Dirac cones [7], which plays a role in stabilizing superconducting [2, 8] and magnetic order [9, 10].

Witt et al. suggested another platform for strongly correlated physics based on graphene with the same strong quantum geometry, but higher intrinsic energy scales and thus also higher critical temperatures for strong correlation phenomena [11]. The model is inspired by an earlier experiment [12] of a SiC(0001) substrate with a single layer of graphene on top and Sn as an intercalant[1] between the substrate and the graphene layer. The system shows signs of Mott-Hubbard bands, a hallmark of strong correlation physics. Witt et al. showed that by using different group-IV intercalants (C, Si, Ge, Sn, Pb) between the graphene sheet and the semiconducting SiC(0001) substrate, different distances to the graphene sheet occur in the ground state. Band structures obtained from Density Functional Theory show a relatively flat band at the Fermi level from the intercalant's $p_z$ orbitals hybridized to the Dirac bands of graphene for all intercalants, with the hybridization strength being tuned by the equilibrium distance of the graphene sheet and the intercalants.

In this thesis I will be treating an elemental model introduced in the work by Witt et al. capturing the essential flat band character of the system. The lattice structure can be seen in fig. 1.1. It consists of a graphene lattice, i.e. a hexagonal Bravais lattice with a two-atom basis [13] (see fig. 1.2a) with an additional atom at one of the sites hosting the flat band. Here, the hopping $V$ models the hybridization.

The interacting model shows two symmetry distinct Mott states for the small and large $V$ regimes: in the low $V$ regime, the X atoms are responsible for the development of local moments, where in the high $V$ limit, the B atoms are responsible. Between these Mott states emerges a metallic state, similar to the topological phase transition of non-interacting bands in the Su-Schrieffer-Heger model [15].

In twisted or untwisted multilayer graphene systems, the energy scale for the emergence of ordered phases is $O(\text{meV})$, corresponding to temperatures of a few K [16, 17].

[1] An intercalant is an atom or molecule inserted between the layers of layered system.

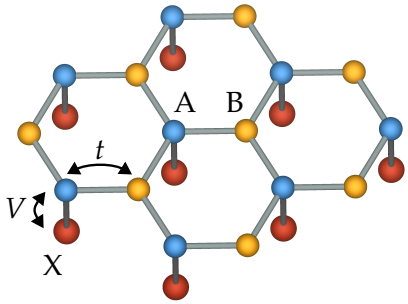


**Figure 1.1 – Lattice structure of the decorated graphene honeycomb lattice.** It has the Graphene hopping $t$ between sublattices A and B as well as the hybridization $V$ between X and A atoms. Created using VESTA [14].

In contrast, the energy scale in this decorated graphene model is set by the hopping $t$, i.e. $O(\mathrm{eV})$ for graphene, so that the correlated flat band physics might persist to higher temperatures.

## 1.1 Lattice Structure

The primitive lattice vectors of the hexagonal lattice are:

$$\mathbf{a}_1 = \frac{a}{2}\begin{pmatrix} 1 \\ \sqrt{3} \end{pmatrix}, \ \mathbf{a}_2 = \frac{a}{2}\begin{pmatrix} 1 \\ -\sqrt{3} \end{pmatrix} \tag{1.1}$$

with lattice constant $a = \sqrt{3}a_0 \approx 2.46\,\text{Å}$, using the nearest-neighbor distance $a_0$, see fig. 1.2a. The vectors from atom $A$ to the nearest-neighbor atoms $B_i$ $(i = 1,2,3,)$ are

$$\delta_{AB,1} = \begin{pmatrix} 0 \\ \frac{a}{\sqrt{3}} \end{pmatrix}, \ \delta_{AB,2} = \begin{pmatrix} \frac{a}{2} \\ -\frac{a}{2\sqrt{3}} \end{pmatrix}, \ \delta_{AB,3} = \begin{pmatrix} -\frac{a}{2} \\ -\frac{a}{2\sqrt{3}} \end{pmatrix}. \tag{1.2}$$

The primitive reciprocal lattice vectors $\mathbf{b}_1, \mathbf{b}_2$ fulfill:

$$\mathbf{a}_1 \cdot \mathbf{b}_1 = \mathbf{a}_2 \cdot \mathbf{b}_2 = 2\pi \tag{1.3}$$

$$\mathbf{a}_1 \cdot \mathbf{b}_2 = \mathbf{a}_2 \cdot \mathbf{b}_1 = 0\,, \tag{1.4}$$

so that

$$\mathbf{b}_1 = \frac{2\pi}{a}\begin{pmatrix} 1 \\ \frac{1}{\sqrt{3}} \end{pmatrix}, \ \mathbf{b}_2 = \frac{2\pi}{a}\begin{pmatrix} 1 \\ -\frac{1}{\sqrt{3}} \end{pmatrix}. \tag{1.5}$$

The first Brillouin zone of the hexagonal lattice is shown in fig. 1.2b, with the points of high symmetry

$$\Gamma = \begin{pmatrix} 0 \\ 0 \end{pmatrix}, \ \mathrm{M} = \frac{\pi}{a}\begin{pmatrix} 1 \\ \frac{1}{\sqrt{3}} \end{pmatrix}, \ \mathrm{K} = \frac{4\pi}{3a}\begin{pmatrix} 1 \\ 0 \end{pmatrix}. \tag{1.6}$$

(a) (b)

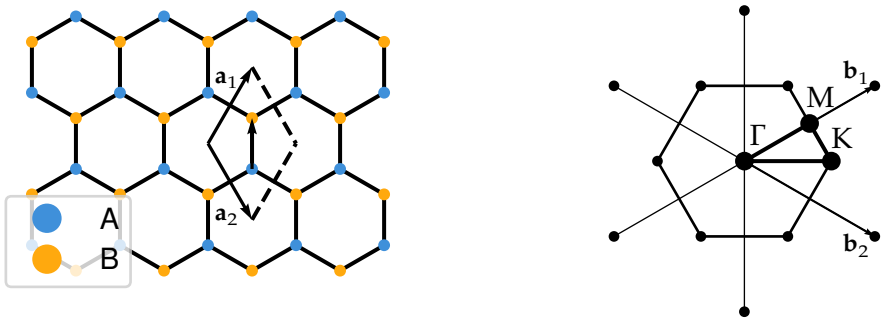


**Figure 1.2 – Graphene lattice structure and Brillouin zone.** (**a**) graphene lattice structure with primitive lattice vectors $\mathbf{a}_1$, $\mathbf{a}_2$ and (**b**) Brillouin zone with reciprocal vectors $\mathbf{b}_1$, $\mathbf{b}_2$. Both images created with lattpy [18].

The elemental model as shown in fig. 1.1 has the following kinetic terms:

$$H_0 = -t \sum_{\langle ij\rangle,\sigma} c_{i\sigma}^{(\mathrm{A}),\dagger} c_{j\sigma}^{(\mathrm{B})} + V \sum_{i\sigma} d_{i\sigma}^{\dagger} c_{i\sigma}^{(\mathrm{A})} + \mathrm{h.c.} \tag{1.7}$$

with operators on the X atom $d$, operators on the graphene sites $c^{(\epsilon)}$ ($\epsilon = \mathrm{A}, \mathrm{B}$), nearest neighbor hopping between graphene sites $t$ and hopping between X and graphene A sites $V$. Using the Fourier transformation

$$c_{i\alpha\sigma} = \frac{1}{N_{\mathbf{k}}} \sum_{\mathbf{k}} e^{\mathrm{i}\mathbf{k}\mathbf{r}_{i\alpha}} c_{\mathbf{k}\alpha\sigma} \,, \tag{1.8}$$

the hopping term becomes

$$-t \sum_{\langle ij\rangle,\sigma} c_{i\sigma}^{(\mathrm{A}),\dagger} c_{j\sigma}^{(\mathrm{B})} \tag{1.9}$$

$$= -t \sum_{i\delta_{\mathrm{AB}}\sigma} c_{i\sigma}^{(\mathrm{A})\dagger} c_{i+\delta_{\mathrm{AB}},\sigma}^{(\mathrm{B})} \tag{1.10}$$

$$= -\frac{t}{N_{\mathbf{k}}} \sum_{i,\sigma} \sum_{\mathbf{k},\mathbf{k}',\delta_{\mathrm{AB}}} \left(e^{-\mathrm{i}\mathbf{k}\mathbf{r}_{i\alpha}} c_{\mathbf{k}\sigma}^{(\mathrm{A})\dagger}\right) \left(e^{\mathrm{i}\mathbf{k}'\mathbf{r}_{i\alpha}+\delta_{AB}} c_{\mathbf{k}'\sigma}^{(B)}\right) \tag{1.11}$$

$$= -\frac{t}{N_{\mathbf{k}}} \sum_{\mathbf{k},\mathbf{k}',\delta_{\mathrm{AB}},\sigma} c_{\mathbf{k}\sigma}^{(\mathrm{A})\dagger} c_{\mathbf{k}'\sigma}^{(\mathrm{B})} e^{\mathrm{i}\mathbf{k}'\delta_{\mathrm{AB}}} e^{\mathrm{i}(\mathbf{k}(\delta_A-\delta_B)+\mathbf{k}'(\delta_A-\delta_B))} \sum_i e^{-\mathrm{i}\mathbf{k}\mathbf{R}_i} e^{\mathrm{i}\mathbf{k}'\mathbf{R}_i} \tag{1.12}$$

$$= -\frac{t}{N_{\mathbf{k}}} \sum_{\mathbf{k},\mathbf{k}',\sigma} c_{\mathbf{k}\sigma}^{(\mathrm{A})\dagger} c_{\mathbf{k}'\sigma}^{(\mathrm{B})} \sum_{\delta_{\mathrm{AB}}} e^{\mathrm{i}\mathbf{k}'\delta_{\mathrm{AB}}} e^{\mathrm{i}(\mathbf{k}(\delta_A-\delta_B)+\mathbf{k}'(\delta_A-\delta_B))} \left(N_{\mathbf{k}}\delta_{\mathbf{k},\mathbf{k}'}\right) \tag{1.13}$$

$$= -t \sum_{\mathbf{k},\sigma} c^{(\mathrm{A})\dagger}_{\mathbf{k}\sigma} c^{(\mathrm{B})}_{\mathbf{k}\sigma} \sum_{\delta_{\mathrm{AB}}} e^{\mathrm{i}(\mathbf{k}\delta_{AB}+2k_y a)} = \sum_{\mathbf{k},\sigma} f_{\mathbf{k}} c^{(\mathrm{A})\dagger}_{\mathbf{k}\sigma} c^{(\mathrm{B})}_{\mathbf{k}\sigma} \ . \tag{1.14}$$

The factor $f_{\mathbf{k}}$ can be written out explicitly using the nearest-neighbor vectors, for example

$$\mathbf{k} \cdot \boldsymbol{\delta}_{\mathbf{AB},\mathbf{1}} = \begin{pmatrix} k_x \\ k_y \end{pmatrix} \cdot \begin{pmatrix} 0 \\ \frac{a}{\sqrt{3}} \end{pmatrix} = \frac{1}{\sqrt{3}} k_y \ . \tag{1.15}$$

This gives:

$$f_{\mathbf{k}} = -t \sum_{\delta_{AB}} e^{\mathrm{i}(\mathbf{k}\delta_{AB}+2k_y a)} \tag{1.16}$$

$$= -te^{2\mathrm{i}k_y a} \left( e^{\mathrm{i}\frac{a}{\sqrt{3}}k_y} + e^{\mathrm{i}\frac{a}{2\sqrt{3}}(\sqrt{3}k_x - k_y)} + e^{\mathrm{i}\frac{a}{2\sqrt{3}}(-\sqrt{3}k_x - k_y)} \right) \tag{1.17}$$

$$= -te^{2\mathrm{i}k_y a} \left( e^{\mathrm{i}\frac{a}{\sqrt{3}}k_y} + 2e^{-\mathrm{i}\frac{a}{2\sqrt{3}}k_y} \cos\left(\frac{a}{2}k_x\right) \right) \ . \tag{1.18}$$

Using the fact that $\delta_{\mathrm{BA},i} = -\delta_{\mathrm{AB},i}$, it follows

$$-t \sum_{\delta_{BA}} e^{\mathrm{i}\mathbf{k}\delta_{BA}} = -t \sum_{\delta_{AB}} e^{-\mathrm{i}\mathbf{k}\delta_{AB}} = \left( -t \sum_{\delta_{AB}} e^{\mathrm{i}\mathbf{k}\delta_{AB}} \right)^* = f^*_{\mathbf{k}} \ , \tag{1.19}$$

which then gives

$$H_0 = \sum_{\mathbf{k},\sigma} C^\dagger_{\mathbf{k}\sigma} \begin{pmatrix} 0 & f_{\mathbf{k}} & V \\ f^*_{\mathbf{k}} & 0 & 0 \\ V & 0 & 0 \end{pmatrix} C_{\mathbf{k}\sigma} \tag{1.20}$$

$$C_{\mathbf{k}\sigma} = \begin{pmatrix} c^{A,\dagger}_{\mathbf{k}\sigma} & c^{B,\dagger}_{\mathbf{k}\sigma} & d^\dagger_{\mathbf{k}\sigma} \end{pmatrix}^T \ . \tag{1.21}$$

For the Hamiltonian in eq. (1.7) at half-filling, there always is a zero-energy eigenstate with a gap separating the other bands from the zero-energy band for any finite value, as shown in fig. 1.3. For $V \to \infty$, the eigenstate is

$$\begin{pmatrix} 0 & 1 & 0 \end{pmatrix}^T \ , \tag{1.22}$$

meaning it is completely localized at the atoms of the non-decorated sublattice B. The maximally localized Wannier function associated with this state is centered and completely peaked in the B sublattice. In the opposite case of $V \to 0^+$, the eigenstate is

$$\begin{pmatrix} 0 & 0^+ & -\frac{f_{\mathbf{k}}}{|f_{\mathbf{k}}|} \end{pmatrix}^T \tag{1.23}$$

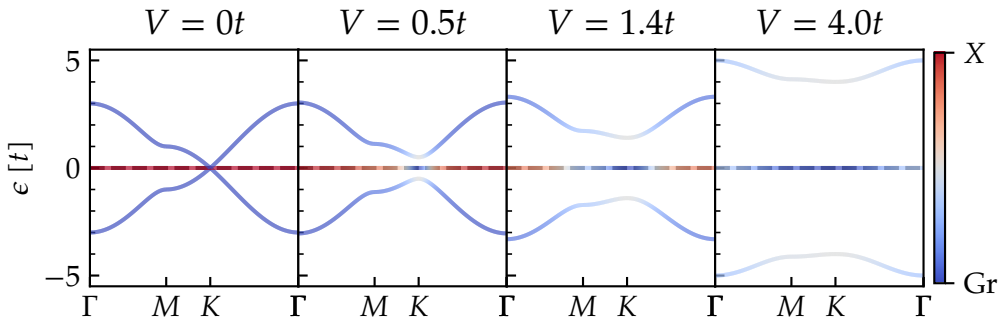


**Figure 1.3 – Decorated graphene band structure.** The orbital weight $W_{\mathbf{k}}$ is marked in color, showing how the flat band switches over from being of X character to being of $\mathrm{Gr_B}$ character when tuning the hybridization $V$.

except for the nodal points where $f_{\mathbf{k}} = 0$. This means that the spectral weight of the flat band is located at the X atoms.

The orbital weight of a Bloch state $|\psi_n(\mathbf{k})\rangle$ corresponding to a band $n$ can be calculated using

$$|w^n_{\mathbf{k}m}|^2 = |\langle\psi_n(\mathbf{k})|m\rangle|^2 \tag{1.24}$$

where $m \in \{\mathrm{Gr_A}, \mathrm{Gr_B}, \mathrm{X}\}$ marks the orbital:

$$|\mathrm{Gr_A}\rangle = \begin{pmatrix}1 & 0 & 0\end{pmatrix}^T,\ |\mathrm{Gr_B}\rangle = \begin{pmatrix}0 & 1 & 0\end{pmatrix}^T,\ |\mathrm{X}\rangle = \begin{pmatrix}0 & 0 & 1\end{pmatrix}^T. \tag{1.25}$$

The orbital character of the bands in fig. 1.3 is calculated via

$$W_{\mathbf{k}} = w_{\mathbf{k},\mathrm{X}} - (w_{\mathbf{k},\mathrm{Gr_A}} + w_{\mathbf{k},\mathrm{Gr_A}})\,. \tag{1.26}$$

It shows how the flat band switches over from being completely of X character to being of $\mathrm{Gr_B}$ character.

## 1.2 Quantum Geometry

Between the edge cases of $V \to \infty$ and $V \to 0^+$, there is no gap closure when keeping $V > 0$, which means that the Wannier center must not have moved. Instead, the maxima of the Wannier centers shift to the three neighboring X sites. As already discussed in **??**, this behavior of the Wannier spread is dictated by the quantum metric. Figure 1.4 shows how the X-orbital weight of the flat band follows the minimal quadratic Wannier function spread [11, 19, 20]

$$\Omega_{\mathrm{I}} = \mathrm{Tr}\, M_{\mu\nu} = \frac{1}{N_{\mathbf{k}}}\sum_{\mathbf{k}} g_{xx}(\mathbf{k}) + g_{yy}(\mathbf{k}) \tag{1.27}$$

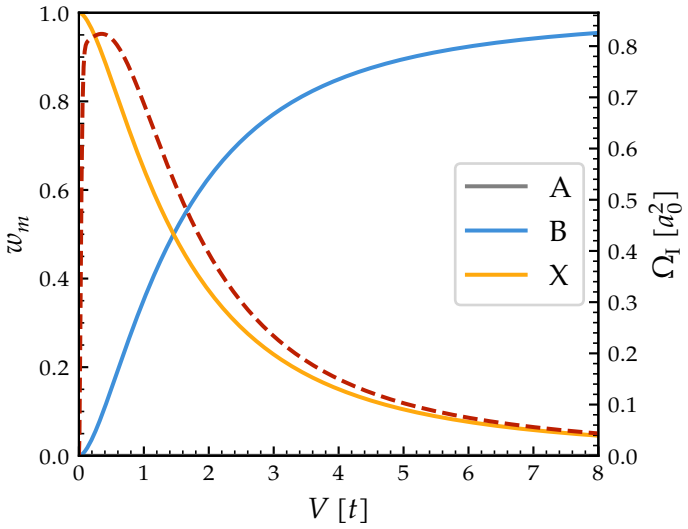


**Figure 1.4 – Orbital weight of the flat band.** The orbital weight is calculated as $w_m = \sum_{\mathbf{k}} |w_{\mathbf{k}m}|^2$ ($m \in \{\mathrm{Gr_A}, \mathrm{Gr_B}, \mathrm{X}\}$) and the quadratic Wannier function spread $\Omega_\mathrm{I}$ is marked as a dotted line.

where $g_{ij} = \mathrm{Re}(Q_{ij}^n)$. It is finite for low $V$ and then going to 0 for large $V$. This mean that following **??**, the model does not support superconductivity for high $V$ because there is no geometric contribution to the superfluid weight at the flat band. For low $V$ there will be a geometric contribution, so superconductivity can be expected in that parameter regime.

The structure of localized orbitals hybridizing with Dirac states is similar to other strongly correlated graphene systems, such as in the heavy Fermion description of magic angle twisted bilayer graphene [21, 22].